Int J Clin Exp Pathol 2017;10(7):7991-7999
www.ijcep.com /ISSN:1936-2625/IJCEP0053951

Original Article

A modified approach to establish a murine model of hypoxic renal interstitial fibrosis

Zhengyuan Cheng, Manoj Hang Limbu, Zhi Wang, Jing Liu, Lei Liu, Xiaoyi Zhang, Pingsheng Chen

Department of Pathology and Pathophysiology, Medical School, Southeast University, Nanjing, Jiangsu, China

Received March 27, 2017; Accepted June 6, 2017; Epub July 1, 2017; Published July 15, 2017

Abstract: Modelling methods that are commonly used to establish a murine model of hypoxic renal interstitial fibrosis mainly includes 5/6 nephrectomy, unilateral ureteral obstruction and cyclosporin A (CsA)-induced renal interstitial fibrosis. The first two methods are technically challenging and unsuitable for clinical practice; thus, CsA induction is more promising. A previously introduced model of CsA-induced renal interstitial fibrosis involves the subcutaneous injection of CsA combined with a 0.01% low-sodium diet. The aim of this study was to provide a modified approach to this model by replacing the subcutaneous injection with gavage and the low-sodium diet with furosemide. From the gross morphology of kidney; the micro-specimens which were stained with haematoxylin-eosin (H&E), Masson-trichrome (Masson), periodic acid-Schiff (PAS); the renal function determination; and the expression of Vimentin protein. Our findings indicate that the combined administration of CsA every day and furosemide every other day by gavage at 80 mg/kg and 60 mg/kg, respectively, for 28 days can be used to successfully establish a murine model of renal interstitial fibrosis. Immunohistochemistry was used to show the expression of renin, the initiator of renin angiotensin aldosterone system (RAAS), while Western blotting was used to show the expression of hypoxia-inducible factor-1α (HIF-1α), a sensitive indicator of hypoxia. The expression levels of renin and HIF-1α revealed that RAAS activation and hypoxia are important mechanisms of this the model. Altogether, the data suggest that our modified approach is also an effective, alternative way to establish this model.

Keywords: Hypoxic, gavage, furosemide, cyclosporin A, renal interstitial fibrosis

Introduction

Due to its increasing prevalence, chronic kidney disease (CKD) has become a worldwide public health problem [1]. Regardless of its cause, CKD ultimately progresses to end-stage renal disease (ESRD), where renal tubular atrophy and interstitial fibrosis are the main pathological changes [2, 3]. Renal interstitial fibrosis is considered the final outcome of CKD. However, the contributing factors of renal interstitial fibrosis are very complex. Fine LG et al. [4, 5] proposed the "chronic hypoxia theory", which suggested that chronic hypoxia in renal tissue is an important factor in the development of renal interstitial fibrosis in CKD. Therefore, establishing a suitable model is crucial to the study of renal interstitial fibrosis and the role of hypoxia. Commonly used modelling methods mainly include 5/6 nephrectomy, unilateral ureteral obstruction and cyclosporin A (CsA)-induced renal interstitial fibrosis. The first two methods are technically challenging and unsuitable for clinical practice; thus, CsA induction may be more promising. CsA is a commonly used drug in clinical practice, and a large body of emerging evidence has associated prolonged CsA administration with the development of severe chronic nephrotoxicity [6, 7]. Thus, a model is required to further study the toxic mechanism of CsA. Furthermore, the pathological changes in the kidney in the CsA model are not only similar to CKD but also consistent with the "chronic hypoxia theory" [8, 9]. Therefore, using CsA to establish a model of renal interstitial fibrosis is more suitable to study the mechanism of CKD and potential treatments.

A previous model of CsA-induced renal interstitial fibrosis in rats was achieved by subcutaneous injection or gavage of CsA [10, 11]. In mice, this model is primarily established by subcutaneous injection of CsA and rarely through gavage [10]. Because mouse genes are highly

homologous to human genes [12], and patients are usually administered CsA orally, we reasoned that a murine model established by gavage would more accurately simulate the clinical presentation of fibrosis.

Earlier studies [13-15] demonstrated that, in addition to CsA, administering a low-sodium diet (0.05% sodium diet for rats and 0.01% for mice; the sodium in a normal diet is approximately 0.4%) is indispensable for establishing a model because low sodium can accelerate the activation of the renin angiotensin aldosterone system (RAAS) and greatly shorten the time required to establish the model successfully. However, the production of a low-sodium diet is time-consuming and expensive, and the standardisation of sodium dosages is difficult. However, furosemide administration can mimic a low-sodium diet because it promotes the excretion of sodium [16]. Thus, we used furosemide instead of a low-sodium diet in mice to provide an alternative way to establish this model.

Materials and methods

Study mice and reagents

The study was approved by the Animal Care Committee of Southeast University (No.2016-0006). One hundred and twenty male ICR mice that were purchased from the Comparative Medicine Centre at Yangzhou University (No. SCXK2012-0004, Yangzhou, Jiangsu, China) were housed in a controlled air, temperature and light environment. The mice were 7-8 weeks old and weighed 30-35 g at the beginning of the experiment. The mice were provided access to a normal diet (Xietong, Nanjing, Jiangsu, China) and tap water throughout the course of the experiment. CsA (ChemBest, Shanghai, China) was diluted to 10 mg/mL in sunflower oil (Arawana, Shanghai, China). Furosemide (Zhaohui, Shanghai, China) was diluted to 10 mg/mL in distilled water.

Experimental design

Mice were randomly assigned to 6 groups of 20 mice each and received the following interventions: Group 1 (G1) received 60 mg/kg furosemide 2 days before the experiment, followed by 80 mg/kg CsA every day and 60 mg/kg furosemide every other day for 28 days. G2 received 80 mg/kg CsA every day for 28 days. G3 initially received 60 mg/kg furosemide 2 days before the experiment, followed by 60 mg/kg furosemide every other day for 28 days. G4 was untreated for 28 days. G5 received sunflower oil for 28 days. G6 initially received distilled water 2 days before the experiment and then every other day for 28 days.

After treatment for 14 and 28 days, metabolic cages (Yuyan, Shanghai, China) were used to collect urine, and 6 mice from each group were anesthetised with isoflurane (Yuyan, Shanghai, China) and sacrificed. Blood was obtained for serum analysis. Kidneys were obtained for tissue histology and Western blotting.

Serum and urine determinations

The serum sodium, creatinine (Scr) and urea nitrogen (BUN) levels in the experimental mice treated with different regimens were evaluated. Whole blood was transferred into a separation gel coagulation tube (BD, Franklin Lakes, NJ, USA), and serum was obtained by centrifugation at 1400×g for 5 min. Serum profiles were determined using a Beckman automatic biochemical analyzer platform (Beckman, Kraemer Boulevard, CA, USA). Urine protein and creatinine were also determined in a similar manner, and then the creatinine clearance rate (Ccr) was calculated using BUN, urine creatinine and urine volume.

Histopathology

The renal pathology of mice treated according to different regimens was evaluated by visualizing tissue sections stained with hematoxylin & eosin (H&E), Masson's trichrome (Masson), and periodic acid-Schiff (PAS) stains. Following euthanasia, the kidneys were immediately removed, photographed, weighed, and fixed with 10% formalin for 24 hours before being embedded in low-melting-temperature paraffin. Paraffin blocks were sliced into 3-μm-thick sections.

H&E staining was used to highlight changes in kidney architecture, and the tubulointerstitial damage index (TDI) was determined according to Shihab et al. [17] Masson staining was used to highlight interstitial renal fibrosis, and the tubulointerstitial fibrosis index (TFI) was evaluated according to Radford et al. [18] Arteriolo-

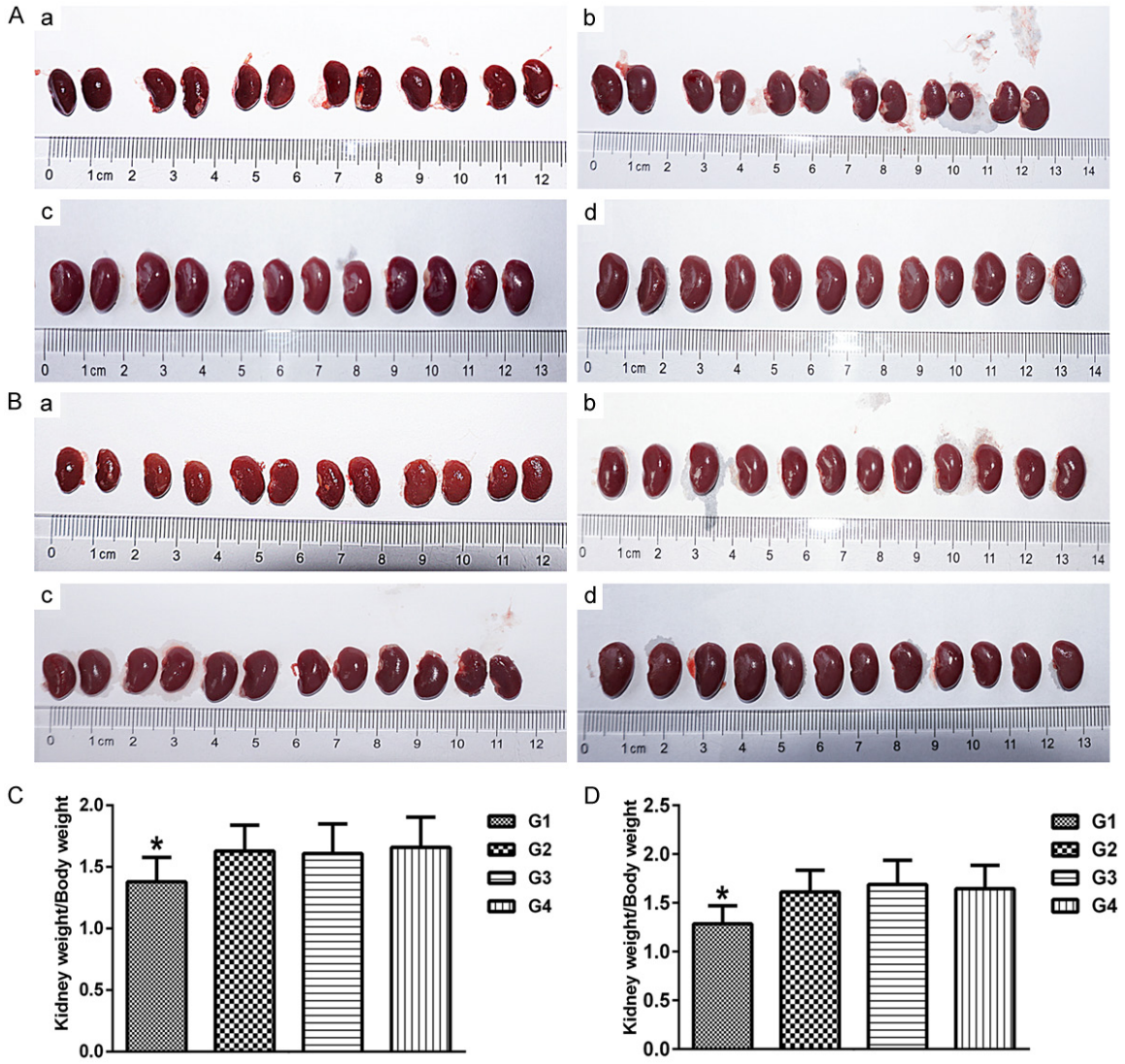

Figure 1. Kidney gross morphology in G1-4 on days 14 and day 28. A. Kidney gross morphology on day 14; a-d. G1-4, respectively. B. Kidney gross morphology on day 28; a-d. G1-4, respectively. C. Kidney-to-body-weight ratio on day 14. *$P < 0.05$ compared with the other groups. D. Kidney-to-body-weight ratio on day 28. *$P < 0.05$ compared with the other groups.

pathy of afferent arterioles was visualized by PAS staining and was calculated according to Li C et al. [19].

Immunohistochemistry

Specimens were immunostained with an anti-renin antibody to reveal renin secretion. First, the specimens were incubated with the anti-renin primary antibody (dilution 1:400; Proteintech, Rosemont, IL, USA) at 4°C overnight, and each slide contained a negative control. Next, the anti-renin primary antibody was visualized using a one-step polymer detection kit (Zhongshan Jinqiao, Beijing, China) according to the manufacturer's instructions. Finally, the results were observed. The staining intensity was quantitated using ImagePro Plus 6.0 (Media Cybernetics, Silver Spring, MD, USA), yielding the intensity optical density/area (area optical density, AOD).

Western blotting

Fresh kidney tissues were collected, lysed, and subjected to protein extraction. Protein concentration was measured by a bicinchoninic acid (BCA) protein assay kit (Beyotime, Beijing,

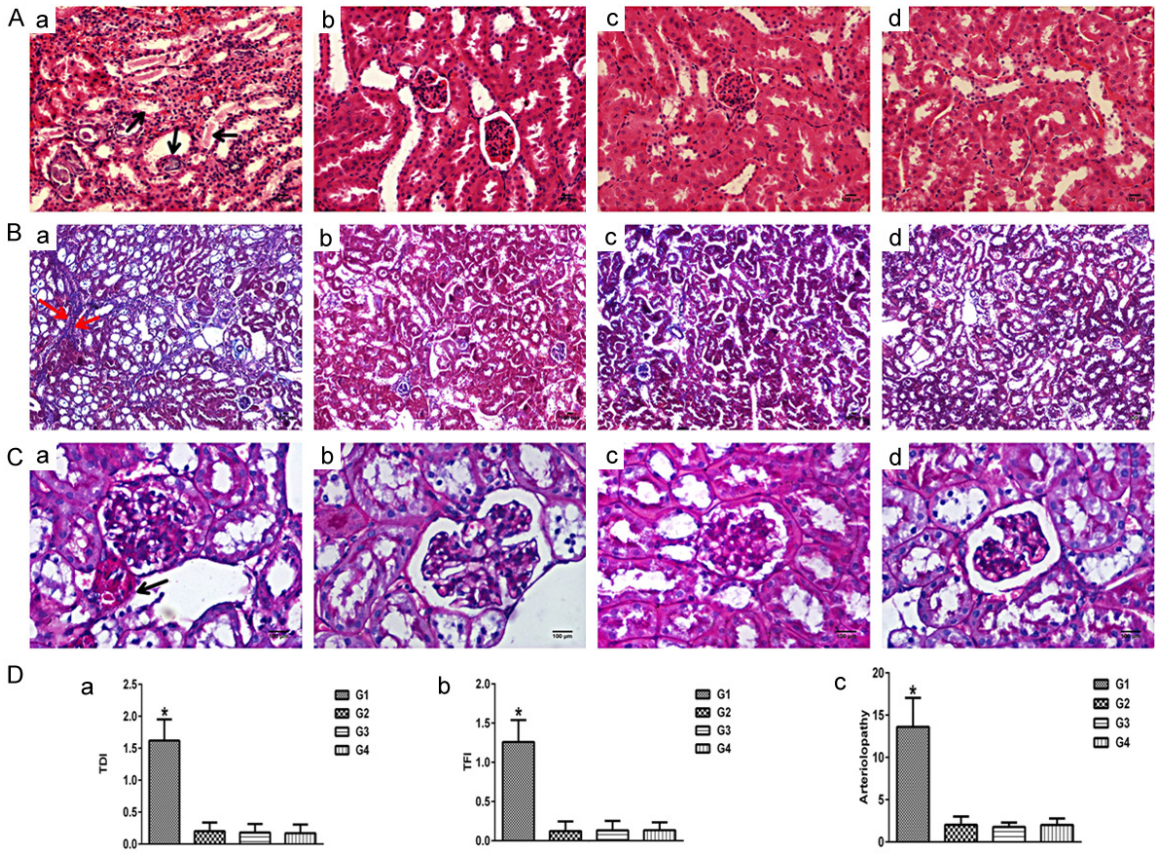

Figure 2. H&E, Masson and PAS stains in G1-4 on day 14. A. H&E (×200); a-d. G1-4, respectively. Arrows denote swelling of the renal tubular epithelial cells, calcium salt and protein casts. B. Masson (×100); a-d. G1-4, respectively. Arrows denote collagen deposition. C. PAS (×400); a-d. G1-4, respectively. Arrows denote arteriolopathy. Da-c. TDI, TFI and arteriolopathy, respectively. *$P < 0.05$ compared with the other groups.

China). The protein expression levels of Vimentin and hypoxia-inducible factor-1α (HIF-1α) were measured by Western blotting analysis. Rabbit anti-human antibodies against Vimentin (Proteintech; dilution 1:1000), HIF-1α (Zhongshan Jinqiao; dilution 1:800) or GAPDH (Proteintech; dilution 1:2000) were used as primary antibodies, and a horseradish peroxidase-linked goat anti-rabbit antibody (Proteintech; dilution 1:3000) was used as secondary antibody. An enhanced chemiluminescence (ECL) imaging method was used to facilitate the detection of protein bands. The experiment was repeated 3 times.

Statistical analysis

Data were expressed as means ± standard deviation. Comparisons between groups were performed using one-way ANOVA with Bonferroni post-hoc correction (SPSS v. 18.0, IBM, Chicago, IL, USA). A value of $P < 0.05$ was considered to be significant.

Results

Morphology

At days 14 and 28, the gross morphology of the renal tissue from the mice in G2-6 (the data of G5-6 are not shown) was full, ruddy, superficially smooth, and had no granular sensation (**Figure 1Ab-d** and **1Bb-d**). By contrast, at day 14, the G1 renal tissue seemed smaller, and the morphology was dark red, superficially rough, and slightly grainy (**Figure 1Aa**). At day 28, the G1 kidneys were noticeably smaller, appeared darker, and had developed a rough, granular surface (**Figure 1Ba**).

The kidney-weight-to-body weight ratio of G1 was markedly decreased compared with that of

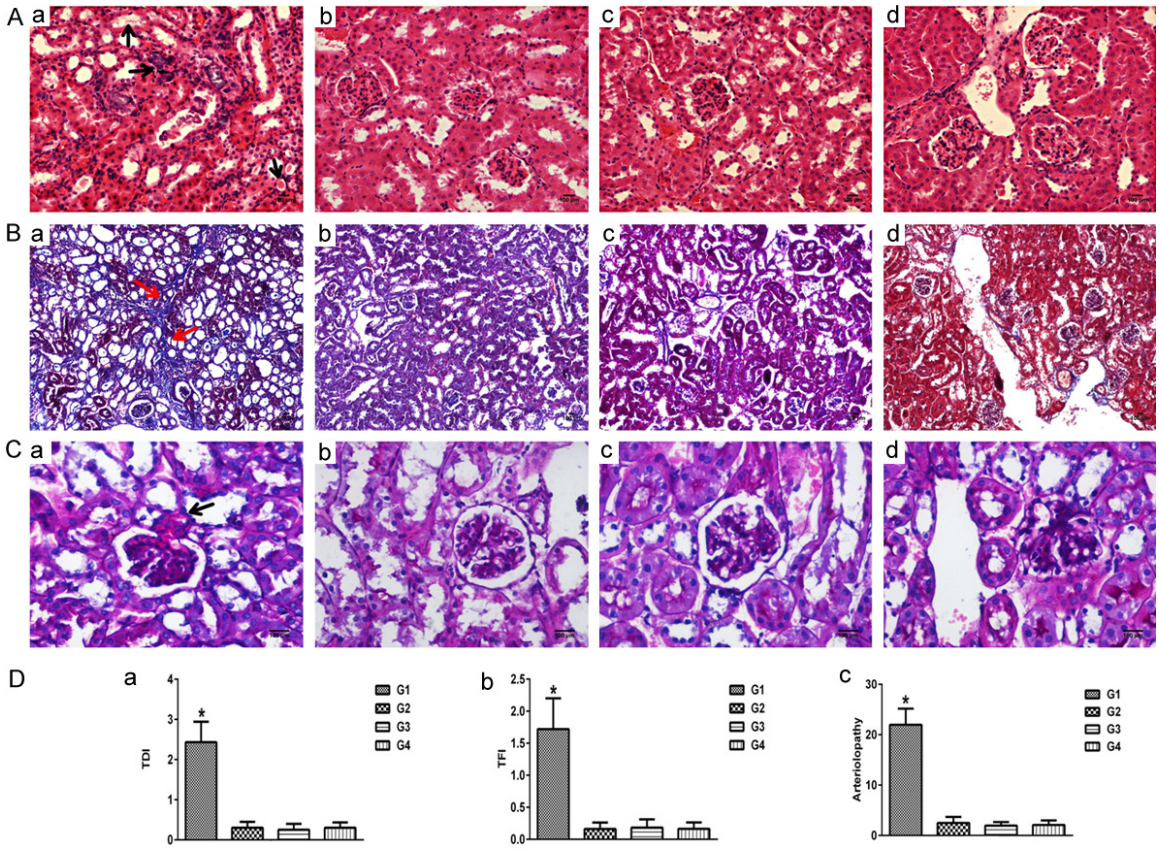

Figure 3. H&E, Masson and PAS stains in G1-4 on day 28. A. H&E (×200); a-d. G1-4, respectively. Arrows denote swelling of the renal tubular epithelial cells, calcium salt and protein casts. B. Masson (×100); a-d. G1-4, respectively. Arrows denote collagen deposition. C. PAS (×400); a-d. G1-4, respectively. Arrows denote arteriolopathy. Da-c. TDI, TFI and arteriolopathy, respectively. *$P < 0.05$ compared with the other groups.

the other groups on days 14 and 28 ($P < 0.05$; **Figure 1C** and **1D**).

Histopathology

Staining with H&E allows for the visualization of tissue architecture, as well as any inflammatory cell infiltration. The renal structures of the mice in G2-6 (the data of G5-6 are not shown) showed no obvious abnormalities on days 14 and 28 (**Figures 2Ab-d** and **3Ab-d**). However, G1 exhibited tubular epithelial swelling and atrophy as well as inflammatory cell infiltration, and the tubular lumen contained calcium salt and protein cast deposits (**Figure 2Aa**). These same parameters were exacerbated on day 28 (**Figure 3Aa**). Additionally, the TDI was evaluated (**Figures 2Da** and **3Da**).

Masson staining highlights interstitial renal fibrosis in renal slices. The renal tissues of G2-6 (the data of G5-6 are not shown) mice were neat, clear, and devoid of collagen deposition (**Figures 2Bb-d** and **3Bb-d**). However, in G1, interstitial renal fibrosis began on day 14 (**Figure 2Ba**) and was more pronounced on day 28 (**Figure 3Ba**). Additionally, the TFI was calculated (**Figures 2Db** and **3Db**).

The presence of renal artery lesions was revealed by PAS staining of the tissue. The examination of the kidneys in G2-6 (the data of G5-6 are not shown) revealed no obvious change in the afferent glomerular arteriolar area on days 14 and 28 (**Figures 2Cb-d** and **3Cb-d**). However, typical afferent arteriolopathy was observed within G1 mice at day 14 (**Figure 2Ca**), which progressed further on day 28 (**Figure 3Ca**). Next, the degree of arteriolopathy was estimated (**Figures 2Dc** and **3Dc**).

Sodium level and renal function

There were no significant differences in the serum and urine sodium levels of mice in G2-6 on days 14 and 28 (**Figure 4Aa**, **4Ab**). However, on day 14, the serum sodium levels of mice in G1 were lower than those in the other groups,

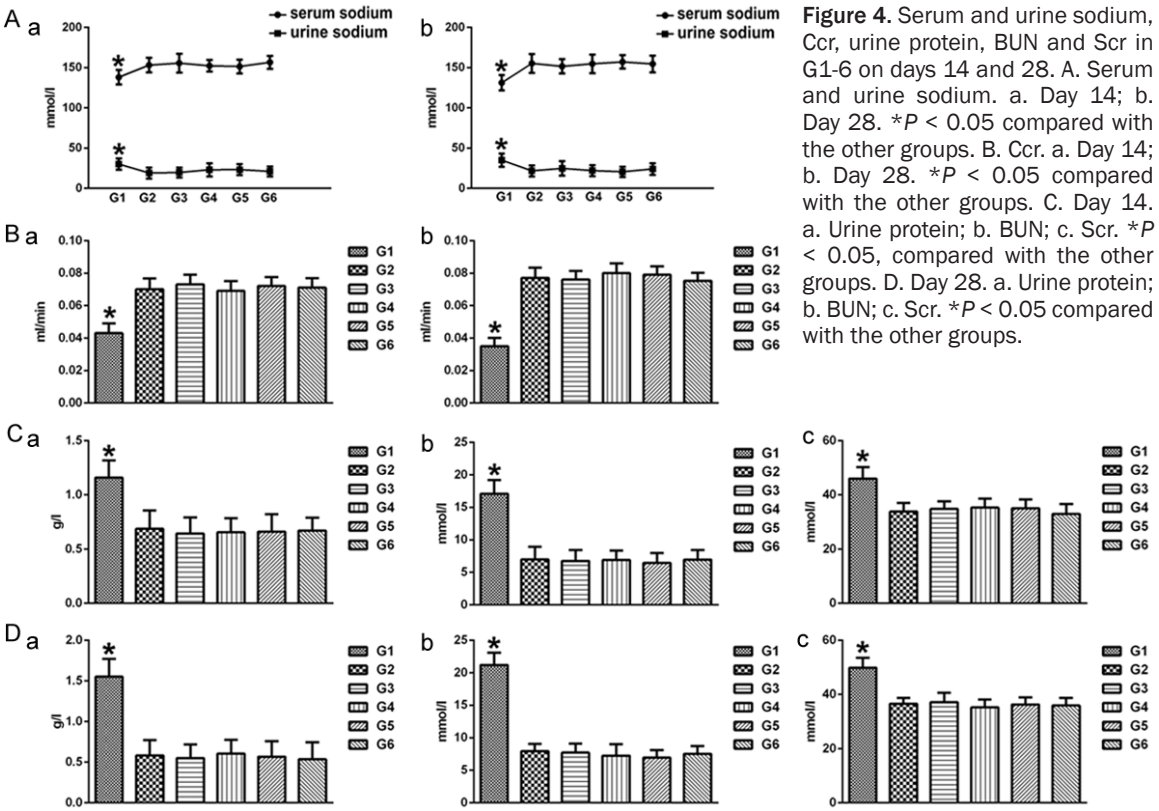

Figure 4. Serum and urine sodium, Ccr, urine protein, BUN and Scr in G1-6 on days 14 and 28. A. Serum and urine sodium. a. Day 14; b. Day 28. *P < 0.05 compared with the other groups. B. Ccr. a. Day 14; b. Day 28. *P < 0.05 compared with the other groups. C. Day 14. a. Urine protein; b. BUN; c. Scr. *P < 0.05, compared with the other groups. D. Day 28. a. Urine protein; b. BUN; c. Scr. *P < 0.05 compared with the other groups.

and the urine sodium levels of mice in G1 were higher than those in the other groups. These profiles on day 28 were more seriously altered than the profiles on day 14 (**Figure 4Aa**, **4Ab**; P < 0.05).

Renal function was assessed by determining the Ccr, urine protein, Scr, and BUN values. On days 14 and 28, there were no significant differences in the Ccr in G2-6 (**Figure 4Ba**, **4Bb**). However, on day 14, the Ccr of G1 was lower than that of the other groups, and on day 28, the Ccr was much lower (**Figure 4Ba**, **4Bb**, P < 0.05). There were no significant differences in the urine protein, BUN or Scr values in G2-6 on day 14 (**Figure 4Ca-c**); however, these indices in G1 were significantly greater than those in the other groups (**Figure 4Ca-c**, P < 0.05). On day 28, there were no significant differences in these indices in G2-6 (**Figure 4Da-c**); however, these indices in G1 were still significantly greater than those in the other groups (**Figure 4Da-c**, P < 0.05).

Immunostaining of the renin

Renin immunostaining of the mouse kidneys in G1-6 (the data of G5-6 are not shown) revealed that positivity labelling was only notable in G1, which was more marked on day 28 than on day 14 (**Figure 5Aa** and **5Ba**). Additionally, the AOD was estimated (**Figure 5C**).

Expression of Vimentin and HIF-1α

Vimentin and HIF-1α expression levels in G1-6 were shown by Western blotting (**Figure 6A** and **6B**). The results revealed that not only on day 14 (**Figure 6Aa** and **6Ba**) but also on day 28 (**Figure 6Ab** and **6Bb**), the expression levels of these two proteins were only observed in G1. In addition, the expression levels of these two proteins relative to GAPDH were estimated (**Figure 6C**).

Discussion

The conventional model of CsA-induced renal interstitial fibrosis relies on the prolonged consumption of a standard, low-sodium diet to induce 'sodium depletion', thereby activating RAAS [12-14]. The activation of RAAS induces renal vasoconstriction, reduces glomerular filtration and renal blood flow, and causes downstream renal ischemic injury; additionally, renal vasoconstriction could exacerbate hypoxia

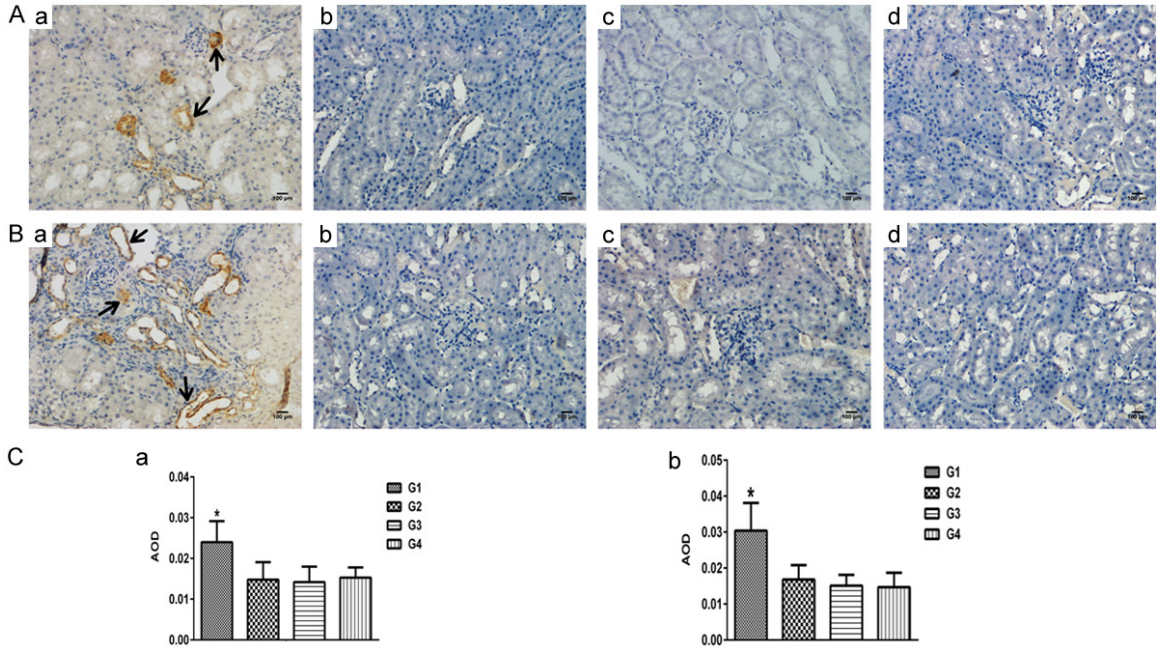

Figure 5. Immunohistochemical staining of renin in G1-4 on days 14 and 28 (×200). A. Day 14; a-d. G1-4, respectively. Arrows denote renin positivity in paracellular cells and vessels. B. Day 28; a-d. G1-4, respectively. Arrows denote renin positivity in paracellular cells and vessels. C. AOD on days 14 and 28; a. AOD on day 14 in G1-4. *P < 0.05 compared with the other groups; b. AOD on day 28 in G1-G4. *P < 0.05 compared with the other groups.

and further aggravate renal tissue injury. These effects can increase the nephrotoxicity of CsA and promote the appearance of renal interstitial fibrosis.

Previous studies have also revealed that the combined use of furosemide and CsA can increase the nephrotoxicity of CsA [20], and the activation of RAAS caused by the induction of low sodium by furosemide may play an important role [13, 14]. Therefore, we sought to establish a murine model by replacing the conventional low-sodium diet with gavage administration of furosemide every other day. However, data regarding the necessary doses of CsA and furosemide to induce this model in mice were not readily available. Thus, based on the quantities of the two drugs used in previous studies [10, 13, 15] and using the equivalent dose conversion table in animals, we first chose doses of 60 mg/kg CsA and 30 mg/kg furosemide; however, after 28 days, the results were negative. We next used 60 mg/kg for both CsA and furosemide, and after 42 days, marked fibrosis began to appear on the kidneys of the mice. We then used 80 mg/kg for both CsA and furosemide, but after 18 days, all mice died. Finally, we chose the present dosage and obtained satisfactory results.

The gross morphology of the kidneys obtained from G1 indicates the onset of fibrosis after 14 days, which became more notable on day 28. By contrast, the mice that received only CsA or furosemide or a range of negative controls showed no obvious signs of fibrosis on days 14 and 28. Furthermore, histopathological analyses of renal sections stained with H&E, Masson, and PAS showed that the kidneys of mice that received CsA and furosemide had tubular atrophy, inflammatory cell infiltration, calcium salt and protein cast deposits, renal interstitial fibrosis, and afferent arteriopathy. By contrast, no notable renal abnormities were observed in the stained kidneys of mice treated with other regimens.

To verify the above pathological results, we detected the serum and urine sodium levels and the related indices of renal function in each group. Unsurprisingly, the combined use of CsA and furosemide exacerbated kidney impairment, as indicated by the significant elevation of the Scr, BUN, and urine protein levels and the reduction of the Ccr level within mice in G1 by days 14 and 28. Additionally, the serum sodium level in G1 on day 14 was lower than that in the other groups, and the urine sodium level on day 14 was higher than that in other groups. On day

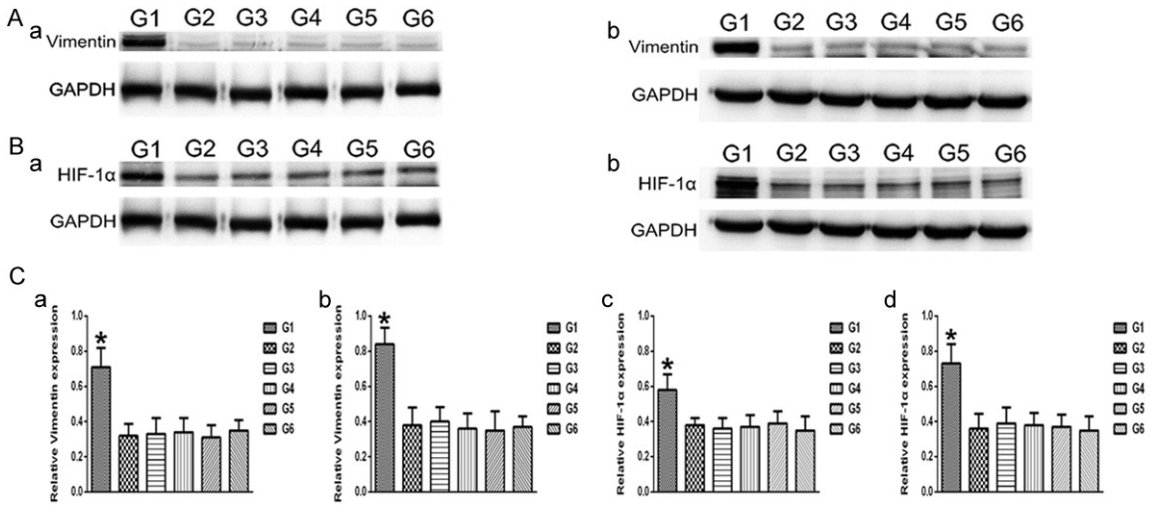

Figure 6. Expression levels of Vimentin and HIF-1α in G1-4 on days 14 and 28. A. Expression of Vimentin; a. Day 14; b. Day 28. B. Expression of HIF-1α; a. Day 14; b. Day 28. C. The relative expression levels of Vimentin and HIF-1α; a, b. The relative expression of Vimentin on days 14 and 28, respectively; c, d. The relative expression of HIF-1α on days 14 and 28, respectively. *$P < 0.05$ compared with the other groups.

28, these changes became more serious. Because furosemide promotes the excretion of sodium, and low sodium can promote the nephrotoxicity of CsA to increase renal tubular injury, the injured renal tubular tissue will further reduce the reabsorption of sodium. Thus, all these effects will lead to increased sodium excretion. In G3, the serum and urine sodium levels on days 14 and 28 were not significantly different from those in G2 or G4-6, likely because the mice in G3 only received furosemide every other day; thereafter, the mice had 48 hours to restore the serum sodium level. Importantly, these data show that single administration furosemide every other day by gavage at 60 mg/kg for 28 days in mice does not induce kidney injury.

Next, we studied RAAS activation in kidney tissue. We studied the production of renin, the initiator of RAAS, and the results showed that on days 14 and 28 in G1, renin was present in paracellular cells and vessels. However, no significant renin distribution was observed in the other groups. This result demonstrates that RAAS activation is an important mechanism of this model.

Finally, we observed the expression levels of Vimentin and HIF-1α by Western blotting. The results showed that these proteins were expressed on days 14 and 28, and there was no notable expression in the other groups. Vimentin is a marker related to the fibrosis, which indicates that fibrosis occurred in G1. In addition, the expression of HIF-1α, a sensitive indicator of hypoxia, demonstrated that hypoxia is an important mechanism of this model.

We demonstrated that a single dose of CsA every day or furosemide every other day by gavage at 80 mg/kg and 60 mg/kg, respectively, for 28 days does not induce kidney injury. However, the combined use of these two drugs accelerates the emergence of renal interstitial fibrosis. Additionally, our experimental results show that the pathological changes in the kidney in the model constructed by our method are the same as those induced by a previous method. These data demonstrate the feasibility of creating a murine model with this method.

However, our method and the traditional widely used method [10, 15] (mice, subcutaneous injection CsA+0.01% sodium diet) may not be perfect, because they both promote increased sodium depletion to accelerate the development of the model. The most ideal method to make the model is with a single use of CsA without any acceleration method (only CsA and normal diet). However, Andoh TF et al. [15] set up a group similar to our G2 and only used a high dose of CsA (100 mg/kg, subcutaneous injection, every day, normal diet, 56 days), and they also did not observe obvious CsA nephrotoxicity. Thus, establishing this model in an

ideal way will be very challenging. Although using accelerated approaches to generate this model do not completely mimic the ideal method, this model will still substantially contribute to the study of renal interstitial fibrosis and the role of hypoxia in this disease.

Acknowledgements

This work was supported by the National Natural Science Foundation of China (No.81-370868).

Disclosure of conflict of interest

None.

Address correspondence to: Dr. Pingsheng Chen, Department of Pathology and Pathophysiology, Medical School, Southeast University, 87 Dingjiaqiao, Gulou District, Nanjing, Jiangsu, China. Tel: (+86) 25-83324887; Fax: (+86) 25-83324887; E-mail: 1642375524@qq.com

References

[1] Romanowski K, Clark EG, Levin A, Cook VJ, Johnston JC. Tuberculosis and chronic kidney disease: an emerging global syndemic. Kidney Int 2016; 90: 34-40.
[2] Levey AS, Coresh J. Chronic kidney disease. Lancet 2012; 379: 165-80.
[3] Meran S, Steadman R. Fibroblasts and myofibroblasts in renal fibrosis. Int J Exp Pathol 2011; 92: 158-67.
[4] Fine LG, Norman JT. Chronic hypoxia as a mechanism of progression of chronic kidney diseases: from hypothesis to novel therapeutics. Kidney Int 2008; 74: 867-72.
[5] Fine LG, Orphanides C, Norman JT. Progressive renal disease: the chronichypoxia hypothesis. Kidney Int 1998; 65: 74-78.
[6] Sang PY. Insights into the possible mechanism of cyclosporine-induced chronic nephrotoxicity; arteriolopathy. Nephrourol Mon 2012; 4: 489-90.
[7] Einollahi B, Teimoori M, Rostami Z. Change of cyclosporine absorption over the time after kidney transplantation. Nephrourol Mon 2012; 4: 70-87.
[8] Yoon HE, Yang CW. Established and newly proposed mechanisms of chronic cyclosporine nephropathy. Korean J Intern Med 2009; 24: 81-92.
[9] Hazzan M, Hertig A, Buob D, Copin MC, Noël C, Rondeau E, Dubois-Xu YC. Epithelial-to-mesenchymal transition predicts cyclosporin nephrotoxicity in renal transplant recipients. J Am Soc Nephrol 2011; 22: 1375-81.
[10] Xiao Z, Shan J, Li C, Luo L, Lu J, Li S, Long D, Li Y. Mechanisms of cyclosporine-induced renal cell apoptosis: a systematic review. Am J Nephrol 2013; 37: 30-40.
[11] Sabbatini M, De NL, Uccello F. Medium-term cyclosporin renal dysfunction and its reversibility in rats. Am J Physiol 1991; 260: 898-905.
[12] Gregory SG, Sekhon M, Schein J. A physical map of the mouse genome. Nature 2002; 418: 743-50.
[13] Rosen S, Greenfeld Z, Brezis M. Chronic cyclosporine-induced nephropathy in the rat: a medullary ray and inner stripe injury. Transplantation 1990; 49: 445-52.
[14] Elzinga LW, Rosen S, Bennett WM. Dissociation of glomerular filtration rate from tubulointerstitial fibrosis in experimental chronic cyclosporine nephropathy: role of sodium intake. J Am Soc Nephrol 1993; 4: 214-21.
[15] Andoh TF, Lam TT, Lindsley J, Alpers CE, Benneti WM. Enhancement of chronic cyclosporin nephrotoxicity by sodium depletion in an experimental mouse model. Nephrol 1997; 3: 471-78.
[16] Watson M. Furosemide. J Exotic Pet Med 2011; 20: 60-63.
[17] Shihab FS, Bennett WM, Hong YI, Choi S, Andoh TF. Sirolimus increases transforming growth factor-β1 expression and potentiates chronic cyclosporine nephrotoxicity. Kidney Int 2004; 65: 1262-1271.
[18] Radford JR, James VD, Bergstralh EJ, Grande JP. Predicting renal outcome in IgA nephropathy. J Am Soc Nephrol 1997; 8: 199-207.
[19] Li C,Yang CW, Kim W, Yung JY, Cha JH, Kim YS, Kim J, Bennett WM, Bang BK. Reversibility of chronic cyclosporine nephropathy in rats after withdrawal of cyclosporin. Am J Physiol Renal Physiol 2003; 284: 389-98.
[20] Whiting PH, Cunningham C, Thomson AW. Enhancement of high dose cyclosporin A toxicity by frusemide. Biochem Pharmacol 1984; 33: 1075-79.